Design Criteria for Star Polymer Formation Processes via Living Free Radical Polymerization

Hugh Chaffey-Millar,[†] Martina H. Stenzel,[†] Thomas P. Davis,[†] Michelle L. Coote,[‡] and Christopher Barner-Kowollik*,[†]

Center for Advanced Macromolecular Design, School of Chemical Sciences and Engineering, The University of New South Wales, Sydney, NSW 2052, Australia, and ARC Center of Excellence in Free-Radical Chemistry and Biotechnology, Research School of Chemistry, Australian National University, Canberra ACT 0200, Australia

Received May 1, 2006; Revised Manuscript Received July 6, 2006

ABSTRACT: The kinetics of reversible addition−fragmentation chain transfer (RAFT), R-group approach star polymerizations have been studied via a combined experimental and theoretical approach. From the improved understanding herein developed, design criteria have been suggested to aid in future syntheses of RAFT, R-group approach star polymer. The suggested criteria are as follows. To minimize the quantity of linear polymer in the system, it is important to have a high rate of monomer propagation but a small delivery of radicals to the system. Crucial to the prevention of star−star coupling and resulting molecular weight distribution (MWD) broadening is the minimization of radical termination events between star molecules. Noting that the number of termination events is directly correlated to the number of decomposed initiator molecules, this might be achieved via several methods. A slow rate of initiator decomposition, a fast rate of propagation, or use of a rate-retarding RAFT agent can all lead to a reduction in star−star coupling events. Additionally, simulations reported herein demonstrate that the use of a star-forming RAFT agent substrate which has a fewer number of arms will lead to a reduction in the concentration of star−star coupled products. Ab initio calculations have been used to study intramolecular RAFT equilibria occurring early in the preequilibrium. These calculations have shown that highly stable intramolecular adduct radicals might be formed due to the close proximity of radicals and S═C bonds. The effect of these on the kinetics is studied.

1. Introduction

The synthesis of complex macromolecular architectures has been revolutionized by the advent of a series of versatile living free radical polymerization methodologies, which allow the polymer chemist to tailor polymers under mild reaction conditions. The most prominent among these are atom transfer radical polymerization (ATRP),[1,2] nitroxide-mediated polymerization (NMP),[3] and the reversible addition−fragmentation chain transfer (RAFT) process.[4−9] These methodologies allow for precise control of the degree of polymerization and the polydispersity of the generated polymer; however, one of their most attractive features is the capacity to generate well-defined star polymer structures. The key idea underpinning the generation of star polymers via living free radical polymerization is that several controlling species are tethered to a central linking moiety which constitutes the core or scaffold of the star polymer (in a core first approach). In the subsequent polymerization process, the polymer chains are inserted between the chain endcap (i.e., the dithioester moiety in the RAFT process, the halide in ATRP, and the nitroxide in NMP) and the core structure. Scheme 1 illustrates this concept in general terms. However, the situation is not as simple as depicted in Scheme 1 in the case of the RAFT process, since one has two principal options for connection of the central core to the RAFT agent; i.e., the core may be connected to the RAFT agent's Z-group (or stabilizing moiety) or to the leaving R-group. The connection of the RAFT agents with its R-group to the core structure is equivalent to the approach required in ATRP and NMP star formation processes.

The connection of the R-group moiety to the core in the case of RAFT (or the connection of the halide or nitroxide in the cases of ATRP and NMP, respectively) has the serious consequence for the polymerization process that the core itself will inevitably carry a radical (or even multiple radicals) and is thus subject to coupling via termination reactions with free propagating radicals, propagating radicals tethered to the core itself, or other radical-carrying cores. Clearly, such coupling reactions are not desirable and can prevent the formation of well-defined polymeric products (or the targeted star polymer) with the amount of coupling products in some cases well exceeding the amount of well-defined star polymer. In an attempt to minimize such coupling products, most studies using ATRP, NMP, and RAFT R-group approaches to stars have only polymerized to low monomer to polymer conversion and/or with low radical fluxes (see for example refs 10−16). In the case of the RAFT process, however, employing a Z-group architecture can avoid the formation of any side products (other than a small amount of dead linear polymer) since the Z-group where chain equilibration takes place is located at the core site and protects the core from undergoing coupling reactions, thus often leading to monomodal molecular weight material, due to the absence of coupled star product.[17,18] However, the approach can be beset with problems in reaching high molecular weight material, since the propagating radicals have to react with the dithioester moiety in order to affect chain extension, which may be difficult to achieve in strongly entangled high-conversion regimes.[19,20] Scheme 2 depicts the nature of the two possible architectural approaches in RAFT polymerization.

[†] The University of New South Wales.
[‡] Australian National University.
* Corresponding author: e-mail camd@unsw.edu.au; phone +61 2 9385 4331; fax +61 2 9385 6250.

10.1021/ma060964w CCC: $33.50
Published on Web 08/19/2006

Scheme 1. Basic Principle of Star Polymer Generation via ATRP, NMP, and R-Group Approach RAFT Systems[a,b]

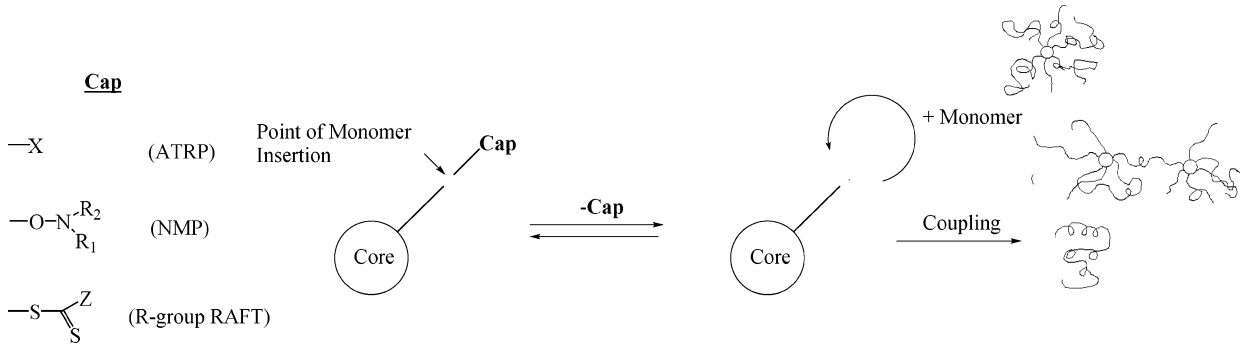

[a] The scheme classifies all three approaches based upon the observation that the central linking core is a radical carrying moiety during the polymerization process. [b] Note that the underpinning mechanistic principles are very different for the RAFT process on one hand and for ATRP/NMP on the other.

Scheme 2. Summarized RAFT Star Polymerization Mechanisms: Z-Group Approach vs R-Group Approach[a,b]

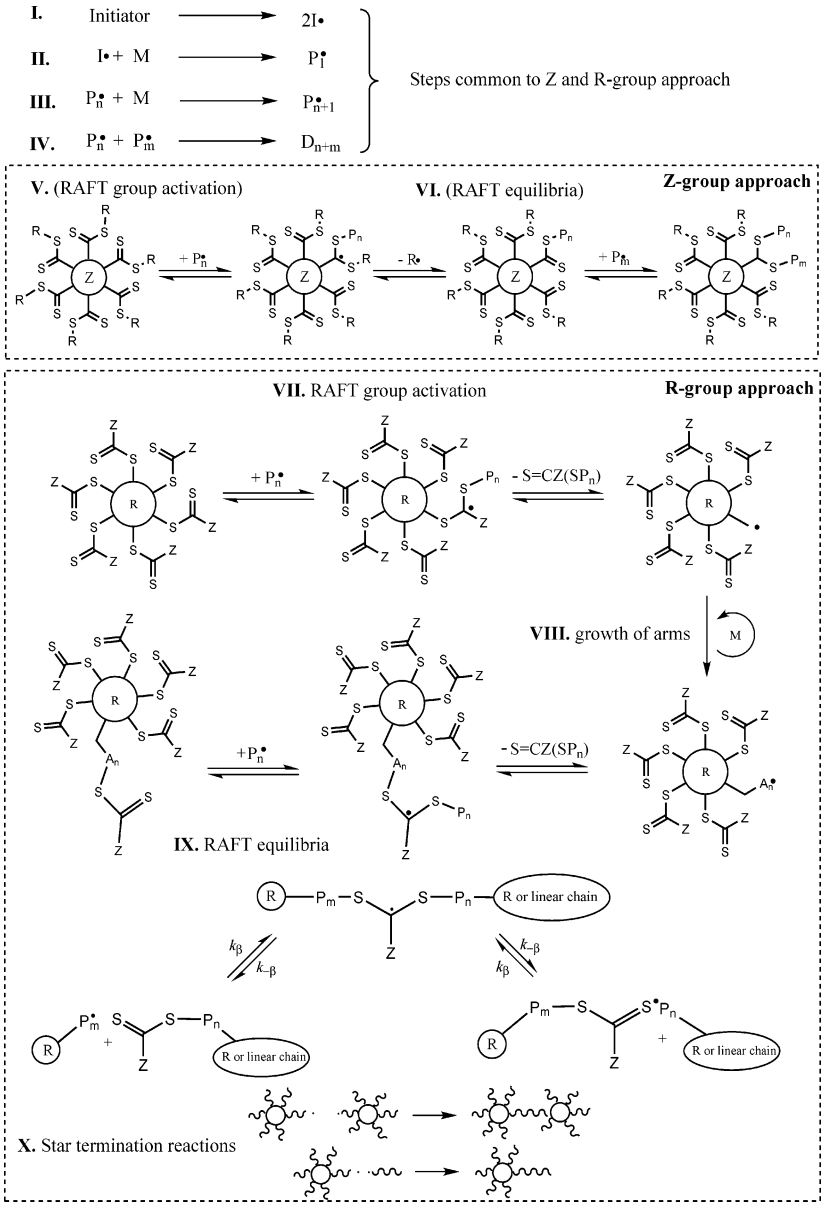

[a] In the Z-group approach, the arms of the star grow as linear chains and are only arms in the true sense when they have undergone additive reaction with the RAFT agent (**VI**). [b] The R-group approach features arm growth on the star proper (**VIII**), with RAFT equilibria taking place between stars and stars, stars and linear chains, or linear chains and linear chains.

While a vast range of star polymers have been prepared by all three of the above methodologies, the parameters that lead to a certain star polymer architecture have not yet been considered in detail and with a mechanistically rigorous approach, especially for the RAFT process. It is thus the aim of the present contribution to rationally map the factors that

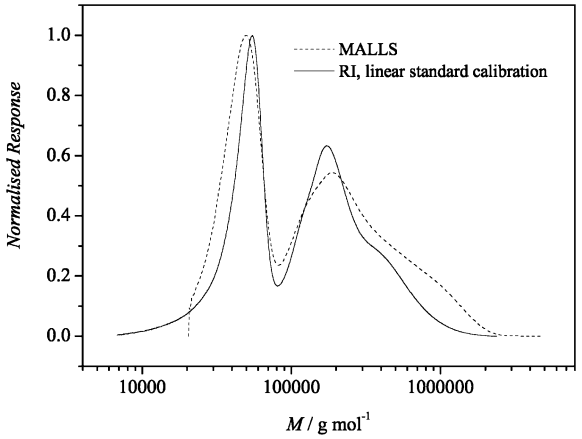

Figure 1. Multiple angle laser light scattering (MALLS) and refractive index (RI) detected GPC traces of a 6-arm styrene star sample, showing close agreement between the absolute molecular weight determination method (LS) and the relative method making use of linear calibration standards. The polymerization leading to this MWD made use of the six-armed RAFT agent depicted in Scheme 3.I ($c_{\text{RAFT groups}} = 0.01$ mol L^{-1}) and azobis(isobutyronitrile) (AIBN, $c_{\text{AIBN}} = 5 \times 10^{-3}$ mol L^{-1}) as the initiator in bulk styrene at 80 °C, proceeding to 45% conversion.

influence star polymer formation and to provide a robust set of guidelines for the preparation of star polymers via the RAFT process. For this purpose, we will analyze complex architecture RAFT polymerization via computational methods while at the same time providing experimental data that underpins the computed predictions. The interplay between theory and experiments thus allows for a set of rational guidelines to be constructed that gives the synthetic polymer chemist who uses RAFT to prepare star architectures, a reference point when deciding on which approach and experimental conditions should be employed.

Recently,[21] we developed a novel computational approach to computation of full molecular weight distributions of star polymers prepared via the RAFT process (and, in principle, other synthetic routes). The approach allows to observe the key parameters of the star polymerization process such as the full molecular weight distributions, the fraction of living star arms, the weight fraction of linear polymer chains, the overall polydispersity of the generated star polymer, and the degree of polymerization of the star polymers among others as a function of the kinetic and experimental parameters. The details of the computational methods will not be reiterated.

In the present study, we will limit ourselves to in-depth discussion of the R-group approach and concentrate to a far lesser extent on Z-group polymerizations. The reason for this is twofold. First, the kinetic computation of Z-group approach star polymer distributions is relatively straightforward since coupling reactions are of minor importance and could only be envisaged through the intermediate RAFT radical at the core site. However, it seems unlikely that such reactions occur to a significant extent.[22−26]

The approach into understanding star polymer formation processes via the R-group approach is three-pronged. Experiments are compared with the results of a novel simulation methodology,[21] and the existence of other reaction processes unique to stars is probed using high-level ab-initio calculations. The kinetic simulations are then used to study the effect of various kinetic parameters on the resulting polymerization.

Styrene star polymerizations have been performed using the three RAFT agents depicted in Figure 1, these being (**I**) 6-arm rate retarded, (**II**) 4-arm rate retarded, and (**III**) 4-arm non-rate retarded. The term rate retarded in this context refers to RAFT

Scheme 3. 6-Arm and 4-Arm RAFT Agents Used in the Preparation of Star-Shaped Polystyrene in This Study[a]

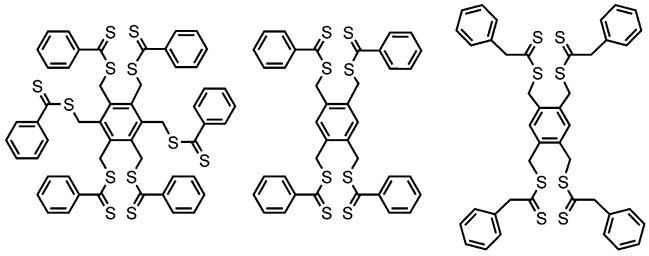

I. 6-arm, retarded **II.** 4-arm, retarded **III.** 4-arm, non-retarded

[a] Agents **I** and **II** display a retarded rate of polymerization while agent **III** displays a non-retarded rate of polymerization.

agents which decrease the rate of conversion of monomer into polymer. The property of being rate retarded is imparted to the substrate S=C(S−R)Z by its possession of a radical-stabilizing Z-substituent. More specifically, turning to the three examples presented in Scheme 3, agents **I** and **II** are rate retarded because Z is a π-stabilizing phenyl group, whereas agent **III** has a benzyl Z-group, which offers a far lesser degree of radical stabilization. The concept of rate retardation is explored in greater depth in ref 27. Simulations of corresponding systems have been performed to verify that the proposed kinetic model is capable of reproducing the qualitative differences between several contrasting systems. The effect of the initial initiator concentration and the relationship between rates of initiator decomposition and rate of propagation have been studied by simulation. Finally, the differences between using rate-retarded and non-rate-retarded RAFT agents are explored. In conclusion, a number of criteria are proposed for consideration when attempting the synthesis of new star polymers using a RAFT R-group approach.

2. Materials and Methods

2.1. Experiment. Polymerizations The required quantities of initiator, RAFT agent, and monomer were thoroughly mixed to achieve homogeneity. Reaction vessels were sealed and the solutions sparged with nitrogen for 15 min. To commence the reaction, reaction vials were placed into isothermal oil or water baths. Sample removal made use of a nitrogen-purged syringe.

Materials. Styrene (Aldrich, 99%) was purified by passing over a column of basic alumina prior to use. 2,2′-Azobis(isobutyronitrile) (AIBN, Aldrich, 99%) was recrystallized twice from ethanol prior to use.

1,2,4,5-Tetrakis(thiobenzoylthiomethyl)benzene, 4-Arm Rate-Retarded Agent.[28] Phenylmagnesium bromide (1.1 equiv) was prepared from bromobenzene and magnesium turnings in dry tetrahydrofuran. Carbon disulfide (1.1 equiv) was added over 15 min, maintaining the reaction temperature at 40 °C. 1,2,4,5-Tetrakis-(bromomethyl)benzene (1 equiv −Br) was added at 40 °C, and then the temperature was increased to 50 °C and maintained for 2 h. Water was added, and the organic products were extracted with toluene, with subsequent rotary evaporation yielding a dark red oil. After dissolution of the dark red oil in chloroform, ethanol was added until the solution became cloudy. A red solid was collected from this solution by precipitation at −18 °C. The red precipitate which formed was recrystallized from a 1:1 ethanol/chloroform solution and dried under vacuum for 2 days. 300 MHz ^{1}H NMR ($CDCl_3$): δ [ppm] = 4.65 (s, 8H, C*H*$_2$−S), 7.33−7.38 (t, 8H, *meta*-Ar*H*), 7.49−7.54 (m, 4H, *para*-Ar*H* and 2H, core-Ar*H*), 7.95 (d, 8H, *ortho*-Ar*H*). ^{13}C NMR ($CDCl_3$): δ [ppm] = 39.2 (*C*H$_2$), 126.9 (*C*H, core-Ar), 128.3 (phenyl-C3), 132.4 (phenyl-C2), 133.4 (phenyl-C4), 134.3 (CS_2C, core-Ar), 144.5 (phenyl-C1), 226.5 (*C*=S). m/z = 764.9 amu; $m/z^{\text{theoretical}}$ = 765.0 amu.

1,2,4,5-Tetrakis(phenylthioacetylthiomethyl)benzene, 4-Arm Non-Rate-Retarded Agent. Benzylmagnesium chloride was formed via a Grignard reaction from benzyl chloride and magnesium metal

in dry diethyl ether. Carbon disulfide was added to the reaction mixture, and the resulting red/brown liquid was refluxed for 1 h and tipped slowly onto ice water. The aqueous phase was collected and washed several times with diethyl ether before acidifying to yield phenyldithioacetic acid which was readily extracted with diethyl ether and evaporated to obtain a yellow oil. An equimolar amount of potassium hydroxide (with respect to dithiophenylacetic acid) was dissolved in a minimum amount of distilled water and added to the dithiophenylacetic acid. The resulting liquid was placed under high vacuum to remove the small amount of water present, yielding potassium dithiophenylacetate as an orange powder. Potassium dithiophenylacetate (1.1 equiv) was dissolved in dry THF before addition of 1,2,4,5-tetrakis(bromomethyl)benzene (1 equiv −Br groups). Heat was evolved, and the reaction mixture was stirred for 1 h. Water was added, and the product was extracted with toluene, which, upon evaporation, yielded yellow crystals. The product was recrystallized from ethanol/chloroform 50:50. 300 MHz ^{1}H NMR ($CDCl_3$): δ [ppm] = 4.27 (s, 8H, CH_2−S), 4.29 (s, 8H, CH_2−CS_2), 7.16 (s, 2H, core-Ar*H*), 7.21−7.36 (m, 20H, 4 × C_6H_5). ^{13}C NMR ($CDCl_3$): δ [ppm] = 38.6 (*C*H_2−S), 57.6 (core-*C*H_2), 127.3 (phenyl-C4), 128.5 (*C*H, core-Ar), 129.0 (phenyl-C3), 132.8 (phenyl-C2), 133.8 (phenyl-C1), 136.5 (*C*CH_2 core-Ar), 233.7 (*C* S_2). *m*/*z* = 820.9 amu; *m*/*z* = 821.6 amu.

1,2,3,4,5,6-Hexakis(thiobenzoylthiomethyl)benzene (6-Arm Rate-Retarded Agent). See refs 11 and 28.

Molecular Weight Characterization. The technique of gel permeation chromatography (GPC) is the primary tool for analyzing the results of polymerizations. It is important to consider, therefore, how the elution characteristics of branched structures might differ from those of linear species of the same molecular weight.

It is well recognized that even with identical molecular weights, branched structures will exhibit a lower hydrodynamic volume than a nonbranched structure due to the former having a higher segment density.[29] This higher segment density arises because the branched structure's chains are tethered. A lower hydrodynamic volume of the branched structure leads to it having a higher GPC elution volume, and as a result its apparent molecular weight (if using linear GPC calibration standards) is lower than its actual value. The elution characteristics of branched polymers vs linear polymers has been studied using a combined experimental and theoretical approach by Radke et al.[13,30] These authors synthesized a range of star structures via several methods. They subsequently performed a comparison of simulated and experimental calibration curves of linear and star polymers, finding there to be semiquantitative agreement between them. As well as normal star polymer, they noted that the dumbbell-shaped star polymer formed (when two star polymers undergo a termination reaction via combination) occur at roughly twice the molecular weight in the chromatogram as compared to normal star polymer.

One way of deobfuscating the differences in elution behavior is to use a detector that measures not only the mass of polymer material eluting at a particular point in time but also the molecular weight of that polymer material. A light scattering detector is able to provide this information in the form of a weight-average molecular weight (M_w) for each differential elution volume element. While there exist the stated differences in the elution characteristics of star as compared to linear polymer, light scattering studies have shown that GPC instruments equipped with refractive index (RI) detectors only (but calibrated with linear standards) are capable of producing chromatograms which are completely adequate for the purposes of this study. A chromatogram of the material resulting from a 6-arm styrene star polymerization is shown in Figure 1. While there are differences, these are mainly in the shape of the high molecular weight shoulder on the main star peak and also slight shifts along the molecular weight axis, the latter being withing the limits of the accuracy of gel permeation chromatography. This implies that we can proceed with using RI detection in the current study, since the objective is to understand the qualitative trends and differences observed in RAFT, R-group approach polymerizations—this is not affected by the stated differences between exclusive RI and multiple angle laser light scattering (MALLS) detection. In the current study, only selected analyses have been performed using MALLS detection (with the others by RI detection and linear standards).

The measurements of MWDs which made use of multiple angle laser light scattering (MALLS) detection employed a Wyatt Technology Corporation Dawn DSP-F laser photometer operating at a wavelength of 632.8 nm with a K5 cell type. The system was equipped with a AS3000 Thermo Separation Products autosampler and a Gynkotek model 300 pump delivering a flow rate of 1 mL min^{-1}. The separation was performed using three columns: PSS−SDV 10^6, 10^5, 10^3 Å (5 μm for each). The eluent was THF at 25 °C.

MWDs involving RI detection only were measured via SEC on a Shimadzu modular LC system comprising a DGU-12A solvent degasser, a LC-10AT pump, a SIL-10AD autoinjector, a CTO-10A column oven, and a RID-10A refractive index detector. The system was equipped with a Polymer Laboratories 5.0 μm bead size guard column (50 × 7.5 mm), followed by three linear PL columns (10^5, 10^4, and 10^3 Å). The eluent was THF at 40 °C with a flow rate of 1 mL min^{-1}. Calibration curves were generated using linear polystyrene standards over a molecular weight range of 500−10^6 g mol^{-1}. The injection volume was 50 μL at 5 mg mL^{-1}).

2.2. Kinetic/MWD Modeling. The method of kinetic modeling[21] involved a kinetic scheme which represented a single arm star. This was simulated using the program PREDICI[31,32] but could in principle have been any method for the simulation of polymerization kinetics, so long as full MWDs are produced and not simply concentrations and average chain lengths.

Such a simulation results in the output of several *fundamental* MWDs, some of which correspond to free/linear chains and others to star bound chains. The MWDs in this latter class are convolved using an iterative algorithm to determine the shape of the MWD of stars formed from these linear chains, i.e., as if they had been joined together all along.

This postprocessing of the fundamental distributions was required for two reasons: (i) straightforward simulation using PREDICI is unable to represent the kinetics of species with many reactive centers and chain lengths, and (ii) it overcomes the overwhelming multitude of reactions to consider when attempting to construct a kinetic scheme for stars.

In the current publication the kinetic modeling method detailed in ref 21 was again employed to simulate star polymerization kinetics; however, several extensions were made to the theory. In ref 21, star−star couples were only treated up to an order of two. In the current work, the method was extended to approximate the MWDs which arise when three or more star species have terminated to form couples. Since star−star coupling is an aberration on the (more desirable) star growth process, it was simulated approximately; that is, the relative amount of e.g. second, third, etc., order couples is *chosen* as a simulation parameter rather than *computed*. This method is described in the Appendix.

Unless specified otherwise, all simulations employed chain length independent rate coefficients and fully implemented preequilibria and core equilibria (i.e., these processes were not implemented as simple chain transfer steps). Table 1 lists the kinetic parameters which, unless specified otherwise, were used in all simulations. While termination rate coefficients are chain length and conversion dependent in reality,[26] it is felt that implementation of this phenomenon in the simulation is unnecessary for the following two reasons: (a) there are no data available on the form that this chain length dependence would take in the case of star/star coupling reactions, and (b) such a modification of the simulations would not change the overall outcomes and trends. Many of the processes explored are so different from that of otherwise equivalent linear polymerizations that the effect of chain length dependence lacks significance by comparison.

Finally, it is important to note that the kinetic model we employ is not intended as an exact replica of the complicated systems of interest. There may be nonrepresented processes such as diffusion-controlled reactions or other entirely new reactions, which are yet to be uncovered. However, this is unlikely to affect the outcomes

Table 1. Kinetic Parameters Used for All Simulations Unless Specified Otherwise (All Values Are for 353 K)

parameter	value	notes
k_i/L mol^{-1} s^{-1}	as for k_p	*a*
k_{ai}/L mol^{-1} s^{-1}	as for k_p	*b*
f	0.64	*c*
k_β/L mol^{-1} s^{-1}	5×10^5	*d*
$k_{-\beta}$/s^{-1} styrene, retarded	0.1	*e*
$k_{-\beta}$/s^{-1} styrene, nonretarded	1×10^5	*f*
$\langle k_t \rangle$/L mol^{-1} s^{-1}	1×10^8	*g*
k_p/L mol^{-1} s^{-1}	630	*h*
k_d/s^{-1}	1.97×10^{-4}	*i*
$\rho_{styrene}$/g L^{-1}	0.870	*j*
$\rho_{vinyl\ acetate}$/g L^{-1}	0.880	*k*
σ/log (g mol^{-1})	0.06	*l*

[c] Initiator efficiency of AIBN in styrene, see ref 33. [d,e,f] These are the generally accepted values for this RAFT equilibrium when slow fragmentation is assumed to be the mechanism of retardation. See for example refs 34 and 21. [g] Various authors have studied the value of $\langle k_t \rangle$ and here an approximate average is chosen; see ref 35 for more information. [h] See ref 36. [i] See ref 33. [j] Density of styrene at 80°C; see ref 37. [k] Density of vinyl acetate at 60 °C; see ref 38. [l] Standard deviation of Gaussian GPC broadening function.

of the present research, since the model has been found to be invaluable as a qualitative tool to understand the general trends which have been observed experimentally.

2.3. Ab-Initio Quantum Mechanical Calculations. On the basis of the structure of the RAFT agents in Scheme 3 and as discussed in greater depth later, it seems possible that intramolecular RAFT equilibria, such as that depicted in Scheme 4, **III** and **IV**, might be occurring in the early stages of the polymerization. It is quite difficult to demonstrate the existence of such a process experimentally, and consequently high-level ab initio quantum mechanical calculations have been performed to probe the feasibility of this mechanism.

Therefore, an approximate equilibrium constant for the ring closure reaction has been calculated. One must be careful with the term equilibrium constant in this context. Since the reactant and product of this reaction are actually different rotational states of the same molecule (radical), a more appropriate term might be the relative populations of the minimum-energy open and minimum-energy closed conformations. However, for familiarity and brevity the term *equilibrium constant* will be used.

The standard equation for calculation of an equilibrium constant or a rate coefficient of a unimolecular reaction from thermodynamic data as well as the general theory of computation of equilibrium constants/rate coefficients from ab initio calculations is described elsewhere.[39,40]

Ab initio molecular orbital theory and density functional theory (DFT) calculations were carried out using GAUSSIAN 98,[41] GAUSSIAN 03,[42] GAMESS-US,[43] and MOLPRO 2000.6.[44] Unless noted otherwise, calculations on radicals were performed with an unrestricted wave function. In cases where a restricted, open-shell wave function was used, it is designated with an R prefix.

Geometries and vibrational frequencies were obtained using the density functional theory (DFT) method B3LYP with a 6-31G(d) basis set. Conformational searches for the global minimum-energy structure were also performed at this level of theory. Improved energies were then calculated, using an ONIOM method[45] to approximate W1[46,47] level of theory energies. This operated by calculating only the core reaction ($CH_3^\bullet + S{=}CH_2 \rightarrow CH_3{-}S{-}CH_2^\bullet$) at the W1 level of theory and then correcting the effect of the substituents using both the high-level composite procedure G3(MP2)-RAD and the lower ROMP2/6-311+G(3df,2p) level of theory. Thus, this three-level ONIOM method (as depicted in Figure 6) consisted of (1) the inner core (above) which was calculated at the W1 level, (2) this small core was then corrected to an outer core using the G3(MP2)-RAD level, making sure that radical centers had all α-substituents present, and then (3) the contribution to the energy from all remaining parts of the molecule was incorporated at the MP2/6-311+G(3df,2p) level of theory. This use of W1 in conjunction with an ONIOM approach has been shown to improve further on G3(MP2)-RAD energies and provide approximate W1 energies. The B3LYP/6-31G(d) optimized geometries are contained in the Supporting Information as Gaussian archive entries. For the rate coefficient calculated, only approximate values were required, and so for these cases a two-layer ONIOM approach was performed in which the G3(MP2)-RAD layer was omitted.

3. Star Polymerization Kinetics: Simulation and Experiment

In this section we describe the effect of a number of polymerization design choices on the resulting molecular weight distributions (MWDs). The features of the MWDs which are of greatest interest include the peak caused by linear chains and MWD broadening caused by coupling reactions. How these effects present themselves are is discussed in terms of initiation, monomer propagation, and RAFT agent structure.

3.1. Formation of Nonstar Material. Linear Chains. It has been observed in previous[11,21,48] and also the current research that the GPC peak due to linear chains (for those systems where such a peak is observed) has living character; that is, its molecular weight increases linearly with conversion. This is indeed what one might expect on the basis of the mechanism and is confirmed by simulation.[21] The reason for the evolution of the molecular weight of this peak with conversion is that the linear chains responsible for this peak have RAFT end groups and are hence living. The MWD of the linear chains in a star system will however differ from that in a linear RAFT system because in the star system the linear chains are all formed from fragments of a slowly decomposing initiator, whereas in a linear RAFT system the chains are initiated by both initiator fragments and R groups which fragment from the RAFT agent.

Star−Star Couples. There are points in need of consideration regarding the role of initiator in star polymerizations. Radical fragments from decomposed initiator molecules give rise to polymer chains that are linear, rather than star like, so it is apparent that an excessive delivery of these species will produce an increased multimodality resulting from (at least) linear polymer impurities. At the outset of the discussions that follow, it is also important to recognize that the number of termination events that occur during a given polymerization can be no more than the number of initiator molecules which have decomposed up until that point. The number of terminated products may possibly be less than the number of decomposed initiator molecules if a radical storage process is in effect; however, this depends on the fate of these radicals upon completion of the polymerization. In the RAFT process, the fate of radicals and possibility of their storage is still an incompletely understood issue and has been the subject of much research.[24,26,49−51]

Since the number of termination events is related to the number of initiator molecules which have decomposed, $I_{decomposed}$, we can expect that if $I_{decomposed}$ is of a similar magnitude to the total number of stars in the system, then a significant degree of coupling will occur, since it is guaranteed that a certain degree of termination events will occur between stars and not only linear chains. This is now demonstrated with an example calculation.

1. As already stated, the number of initiator molecules gives an upper bound to the number of terminated products, i.e.

$$c_{term'ed\ prod's} \leq c_{I,0} - c_I \qquad (1)$$

where c_x denotes the concentration of substance x.

2. If each star has 6 arms, then there are 6 RAFT (dithioester) groups per star.

3. Commonly, one might use a RAFT agent concentration that is 10 times the initiator concentration,[34,49] i.e.

$$c_{\mathrm{RAFT},0} = 10c_{\mathrm{I},0} = 6c_{\mathrm{stars}} \quad (2)$$

due to point 2.

4. If all radicals are removed from the system by a termination mechanism *and* there is the condition of high initiator conversion, then

$$c_{\mathrm{I},0} - c_{\mathrm{I}} \approx c_{\mathrm{I},0} \quad (3)$$

and since a single initiator molecule leads to two initiator halves, the concentration of couples is given by

$$c_{\mathrm{couples}} = 2fc_{\mathrm{I}}$$

where $f = 0.64$ is a typical initiator efficiency.[33]

5. An expression for the fraction of stars which have coupled to something, if all termination had occurred between stars, is

$$\text{couple fraction} = c_{\mathrm{couples}}/c_{\mathrm{stars}} = \frac{2fc_{\mathrm{I}}}{10c_{\mathrm{I}}/6} = \frac{12f}{10} \approx 0.8$$

It can be seen that in this example scenario a single star molecule has a probability of being connected to another one of 0.8. Some stars will of course have no coupling, but others will have more than one.

It is possible to obtain a more general expression for the star coupling fraction and evaluate this using simulated data. The expression obtained is eq 4.

$$\text{couple fraction} = \frac{2ac_{\text{coupled species}}}{c_{\mathrm{RAFT},0}} \quad (4)$$

In eq 4, a is the number of arms, $c_{\text{coupled species}}$ is the concentration of coupled species, and $c_{\mathrm{RAFT},0}$ is the initial RAFT group concentration. This expression has been evaluated for simulated rate-retarded and non-rate-retarded star polymerizations, for 4- and 6-arm stars. Its value is plotted as a function of monomer conversion in Figure 2. The simulation leading to Figure 2 was parametrized for an AIBN initiated styrene star polymerization at $T = 353$ K with $c_{\mathrm{AIBN}} = 2 \times 10^{-3}$ mol L^{-1}, $c_{\mathrm{RAFT}} = 1 \times 10^{-2}$ mol L^{-1}, and $k_{-\beta} = 1 \times 10^{5}$ or 1×10^{-1} L mol^{-1} s^{-1} depending on whether the system was non-rate retarded or rate retarded, respectively.

Concentrating first on the differences between 6- and 4-arm stars, it can be seen in Figure 2 that there is an increase in the degree of coupling as the number of arms increases (but the RAFT group concentration is held constant). This is because the same number of couples is shared among a smaller number of stars. Second, there is also a significant difference in the resulting degrees of coupling for rate-retarded vs non-rate-retarded star polymerizations. Under the assumption that rate retardation is caused by slow fragmentation (i.e., β-scission of a $-$S$-$C$^{\bullet}$(Z)$-$S$-$ species) rather than cross-termination,[22−26,51] this phenomenon will lead to a reduction in the number of termination events during the polymerization. This implies that

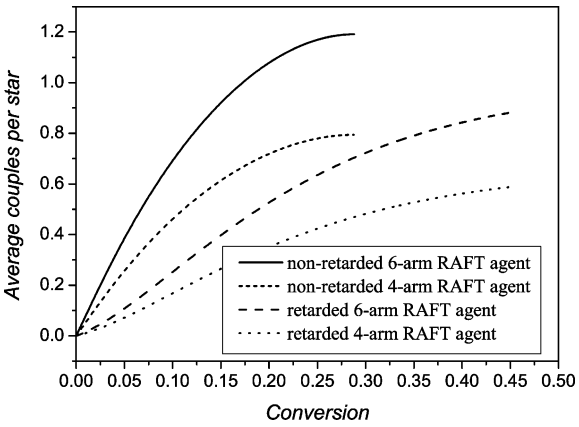

Figure 2. Couple fraction as a function of monomer conversion for four systems (from top to bottom): non-rate-retarded 6-arm, non-rate-retarded 4-arm, rate-retarded 6-arm, and rate-retarded 4-arm. The simulated system was an AIBN-initiated styrene star polymerization at $T = 353$ K with $c_{\mathrm{AIBN}} = 2 \times 10^{-3}$ mol L^{-1}, $c_{\mathrm{RAFT\ groups}} = 1 \times 10^{-2}$ mol L^{-1}, and $k_{-\beta} = 1 \times 10^{5}$ or 1×10^{-1} L mol^{-1} s^{-1} depending on whether the system was non-rate retarded or rate retarded, respectively. All other simulation parameters as in Table 1.

at any given conversion a non-rate-retarded system will have experienced more termination events than an equivalent rate retarded system due to radical storage. This leads to a significant difference in the degree of coupling between these two systems, and in Figure 2, at 20% conversion, the non-rate-retarded systems have approximately 2−3 times the degree of coupling as the same arm number rate-retarded systems. If cross-termination *was* the cause of retardation, eq 4 would require redefinition, and there would be very little if any difference between the curves for rate-retarded and non-retarded-systems in Figure 2. As will be demonstrated and discussed in a later section, the use of a rate-retarding RAFT agent leads to a decrease in the number of star−star couples as compared to a non-rate-retarding RAFT agent, and this is in agreement with (a) the simulation results of Figure 2 and (b) the notion that cross-termination which occurs throughout the polymerization is somewhat unlikely to have significant importance for the kinetics of these systems.

Lower Molecular Weight Starlike Polymer. Star material formed by polymerization using RAFT agent (I) in Scheme 3 features a low molecular weight shoulder on the peak due to ideal star material (see Figure 3). While this feature of star polymerization kinetics is not of central importance, it is important to consider mechanisms for the shoulder's origin. There are a number of possible mechanistic origins of such a peak, some of which have been suggested in the past[11,21] and others which have been the subject of the current study (and several fall into both categories). The mechanistic origins responsible might (in a broad sense) include (but may not be limited to) (a) an incompletely functionalized RAFT agent sample, (b) biradical termination reactions between star and linear polymer radicals, (c) intramolecular termination reactions between radical bearing star arms, (d) the effect of the small fraction of termination reactions which occur via disproportionation rather than termination (∼10%),[52] or (e) some other termination event which stops arm growth early in the polymerization.

Point (a) can be ruled out using standard organic compound characterization methods. The ^{1}H NMR spectra obtained have peak integrals indicative of a high-purity product. For this to be a cause of the low MW shoulder observed, there would need to be a significant fraction of unfunctionalized RAFT groups

in the RAFT agent sample. Additionally, the two hydrogens present between the central aromatic ring and the sulfur in agent **I**, Scheme 3, i.e., $C_6(CH_2-\mathbf{X})$, have a chemical shift in ^{1}H NMR highly dependent on the identity of **X**. Since only a single peak is observed in the ^{1}H NMR spectrum of agent **I**, Scheme 3, it is extremely unlikely that a significant number of arms are unfunctionalized. (In the case of $\mathbf{X} = S-C(=S)Z$ a singlet at $\delta = 4.66$ ppm is observed, whereas for $\mathbf{X} = Br$ a singlet at $\delta = 4.7$ ppm is observed.)

It has been found in the current and previous[21] study that material formed by the process described in point (b) creates star material whose MWD is essentially indistinguishable in molecular weight from that of so-called normal star material. This finding comes from the observation that low molecular weight shoulders never appear in the simulated MWDs even though the linear polymer−star polymer terminations are always implemented in the simulations.

Intramolecular termination reactions, point (c), seem very unlikely since our modeling studies have shown that the probability of a star molecule bearing two radicals simultaneously is small. To see this, consider a 2-arm star. The concentration of radical arms is of the order 10^{-8} mol L^{-1}. If the concentration of RAFT groups, i.e., arms in the system, is 1×10^{-2} mol L^{-1}, then the probability, $P(^{\bullet}S^{\bullet})$, of a star bearing two radicals simultaneously is given by $P(^{\bullet}S^{\bullet}) = c_{star}P(A^{\bullet})^2$, where $P(A^{\bullet}) = 10^{-8}$ mol L^{-1}/10^{-2} mol L^{-1} $= 10^{-6}$ is the probability that a single arm bears a radical and c_{star} is the concentration of stars. Hence, $P(^{\bullet}S^{\bullet}) = 10^{-12}$. While the concentration of intramolecularly terminated products depends on the unimolecular and diffusion-controlled rate coefficient for this intrachain reaction, it seems unlikely that the rate could ever overcome the low concentration of the required starting product. (Much work has been done on the subject of intrachain termination reactions;[53−56] however, a full discussion of this is beyond the scope of the current study.)

In consideration of (d), simulations (the results of which are not depicted) have been performed to assess whether the shortened arms on stars due to disproportionation could possibly create a significantly different molecular weight product, and it has been found that this mechanism only leads to very subtle low molecular weight shoulders on the main peak.

It needs to be mentioned that points (c) and (d) lead to products that are formed continuously during the course of the polymerization and that, in general, this will not create a product of significantly lower molecular weight than normal stars. Consequently, it is suggested that the most plausible explanation is a process which occurs early during the polymerization (and only at this time) which prevents these arms from growth for the rest of the polymerization. This idea is discussed in greater detail later, and we tender a hypothesis on the type of process which might be responsible.

3.2. Effect of Propagation Rate. The CAMD group[11] has previously produced styrene star polymer containing material using an R-group approach synthetic attempt. They employed the RAFT agent depicted in Scheme 3.I to mediate thermally initiated styrene at 100 and 120 °C as well as AIBN-initiated styrene at 80 °C. The crucial features of the resulting molecular weight distributions were, proceeding from low to high molecular weight, (1) a peak due to free chains, (2) a low molecular weight shoulder on the main peak, (3) a main peak due to the ideal star material, and (4) a high molecular weight shoulder on this main peak.

Through experimental and simulatory work that is the subject of the current study, it has been found that, by polymerizing the same system under conditions of reduced temperature, more structured distributions are obtained. That is, at lower temperatures, the peaks due to material other than strictly star-shaped polymer become more prominent. We will demonstrate below that this phenomenon is related to the comparative rates of initiator decomposition and monomer propagation.

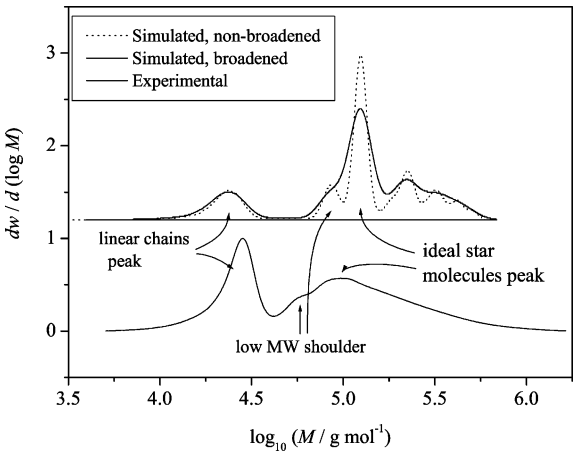

Figure 3. Selected simulated (top) and experimental (bottom) data from a RAFT, R-group approach 6-arm styrene star polymerization (bulk) at 353 K, initiated with AIBN. The experimental sample and simulation data are presented for polymerization to 24% conversion: $c_{\text{RAFT groups}} = 1 \times 10^{-2}$ mol L^{-1} and $c_{\text{AIBN}} = 1.95 \times 10^{-3}$ mol L^{-1}. As indicated in the above figure, a low molecular weight shoulder on the peak due to ideal star material appears in the simulated GPC trace. This appears because the termination mechanism described later was implemented when generating this simulated data. See section 3.3 for further discussion. The linear chains peak arises from polymer chains which have grown from (monofunctional) initiator fragments rather than (hexafunctional) RAFT agent molecules. The figure demonstrates how the simulations reproduce the structuring of the MWDs, a feature which arises due to the styrene system having a relatively low rate of propagation but a relatively high rate of initiator decomposition.

Vinyl acetate (VA) has a faster rate of propagation compared to styrene (at 60 °C, k_p/L mol^{-1} s^{-1} = 9460[58] vs 340[36]), and this has important repercussions for the comparative kinetics of these two systems. In previous work, the CAMD group[19] have polymerized VA in the presence of a 4-arm, xanthate-based R-group approach RAFT agent and reported largely monomodal and nonstructured MWDs—in contrast to what is observed for styrene under similar conditions. It is shown via simulation in this section that this can be explained by the significantly differing propagation rate coefficients of these two monomers.

Figures 3 and 4 depict experimental and simulated MWDs for a 6-arm styrene star polymerization at 80 °C and a 4-arm vinyl acetate star polymerization at 60 °C, respectively. Table 2 contains the conditions as well as rate coefficients used for the experiments and simulation. Unless it was sought to examine the effect of disproportionation vs combination, termination reactions in both simulations were modeled as occurring exclusively via combination. While it is known that for styrene combination is favored by ≈90%, the termination kinetics of VA are less clearly understood. However, in the VA system, since termination reactions occur to a far lesser extent, it was found that the mode of termination makes almost no difference to the MWDs. The main objective of the VA simulations was to show that monomodal distributions are produced; this occurs regardless of the termination mode chosen for the simulation. It has been found that the monomer reaction order in this system is close to unity,[38] indicating a low occurrence of midchain radicals. It is also known that the transfer constant for transfer to monomer is merely 2×10^{-4} at 60 °C.[57] Thus, in the VA

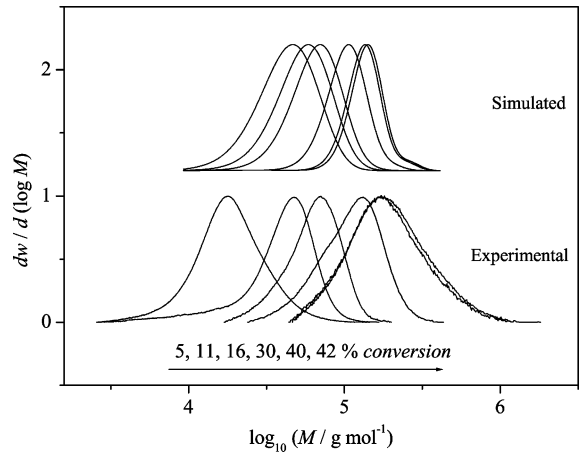

Figure 4. Selected simulated (top) and experimental (bottom) data from a RAFT, R-group approach 4-arm vinyl acetate star polymerization (bulk) at 333 K, initiated by AIBN. $c_{AIBN} = 2.2 \times 10^{-3}$ mol L^{-1} and $c_{RAFT\ groups} = 4.4 \times 10^{-2}$ mol L^{-1}. The experimental data come from a study by Bernard et al.[19] The figure demonstrates how the simulations reproduce the monomodal MWDs seen in the experiments, a feature which arises due to the VA system having a relatively high rate of propagation but a relatively low rate of initiator decomposition.

Table 2. Parameters and Conditions Applicable to the VA and Styrene Experiments and Simulations Which Are the Subject of Figures 3 and 4

	monomer			
	styrene	notes	vinyl acetate (VA)	notes
k_p/L mol^{-1} s^{-1}	630	*a*	9460	*b*
k_d/s^{-1}	1.97×10^{-4}	*c*	1.46×10^{-5}	*c*
T/K	353		333	
c_{AIBN}/mol L^{-1}	1.95×10^{-3}		2.2×10^{-3}	
c_{RAFT}/mol L^{-1}	1×10^{-2}	*d*	4.4×10^{-2}	*d*
arms	6		4	

[a] See ref 36. [b] See ref 58. [c] See ref 33. [d] Refers to the concentration of RAFT groups, not the concentration of RAFT agent.

model and, for that matter, the styrene model, no transfer to monomer or polymer was implemented, since the level at which it occurs is unlikely to significantly affect the MWDs.[34]

There are some differences between the experimental and simulated data in both systems, and it is important to discuss these. For the styrene system, the experimental MWD appears less structured than the simulated one. It may be that a greater degree of GPC column broadening is operative for the star material, and the differences are entirely due to separation effects. It is also possible that there are additional kinetic processes present which were not represented in the model and that these give less distinct peaks in the MWD. An example of such a process might be altered addition and β-scission rate coefficients for intra- and intermolecular RAFT reactions. The vinyl acetate polymerizations resulted in molecular weight distributions which are at times broader than the simulated ones. It was pointed out by those authors[19] that there might have been some loss of control at higher conversions. They also observed an inhibition period which was not attributed to inhibition by the RAFT agent, but rather minute quantities of impurity in the polymerization,[59,60] which, due to the high reactivity of the propagating p(VA) radical, were able to react with and prevent propagation of the p(VA) radicals, quenching the polymerization.

Interplay between k_d and k_p. Since reactions such as those leading to star−star coupling do not affect the relative proportion of branched and linear polymer material produced, it is possible to derive a mass fraction of branched (as opposed to linear) polymer as a function of both k_p and k_d. This is plotted as a surface in Figure 5. From this figure it can be seen that in general an increasing propagation rate coefficient leads to an increase in the selectivity toward starlike material, since the total reaction time is shorter and less linear chain forming initiator has decomposed. Several experimental systems have been placed on the surface. These are vinyl acetate (VA)/AIBN at 60 °C, styrene/AIBN at 60 °C, styrene/AIBN at 80 °C, and styrene/autoinitiation at 100 °C. Only four examples have been placed on the surface in Figure 5—while there are other examples in the literature of RAFT R-group approach star polymerizations, these are lacking sufficient similarities to be placed on the surface depicted due to, for example, significantly architectural differences[61] or experimental conditions.[48]

Thus, it may be considered desirable to increase the propagation rate coefficient as much as possible, provided the system does not reach the desired conversion before (a) all the RAFT groups have been activated or (b) stars have disparate arm lengths.

3.3. Reactions during the Preequilibrium. It seems possible that the close proximity of reaction centers might alter the kinetics which are operative in star as compared to linear RAFT polymerizations. In particular, intramolecular RAFT equilibria at very short chain lengths would be expected to be affected the greatest. To probe this, high-level ab-initio calculations have been performed.

It is expected that a slower preequilibrium, i.e., one in which the initial RAFT agents are activated slowly, results in broader molecular weight distributions, since the main population of chains contains species whose activations take place over a longer time period. It seems possible therefore that there are additional processes taking place in systems with a multifunctional RAFT-agent mediated polymerization which affect the way the system moves through the preequilibrium stage. More specifically, it seems possible that intramolecular RAFT equilibria, such as the one depicted in Scheme 4, might be active. If the seven-membered ring structure (Scheme 4.IV) were to be formed in sufficiently high concentration, then it might be possible for a cross-termination reaction such as that in Scheme 4.V to take place and create the observed low molecular weight shoulder on the main star peak in experimental MWDs.

To gather evidence as to whether such a reaction is possible, high-level ab-initio calculations have been performed to calculate the equilibrium constant for the reaction depicted in Scheme 5.

The constant of the equilibrium in Scheme 4 has been found to be approximately 3×10^6 at 333 K and 1×10^6 at 353 K (to make sure that the reaction is capable of occurring, that is, the activation energy is not too high, an approximate addition rate coefficient, k_{close}, has been calculated using an ONIOM system in which the G3(MP2)-RAD layer (Figure 6) was omitted. This gave a value of $k_{close} \approx 1 \times 10^7$ s^{-1} at 353 K, implying that the ring closure reaction is certainly feasible.) While an equilibrium constant of $\approx 10^6$ may seem inconsequential given that several studies report the magnitude of the equilibrium constant of a bimolecular RAFT equilibrium to be at least this,[24,27,62] the fact that it is a unimolecular process means that the fused ring structure enjoys a far higher population than the adduct of a bimolecular process with the same equilibrium constant and S═C group concentration. To see this, consider that the rates for

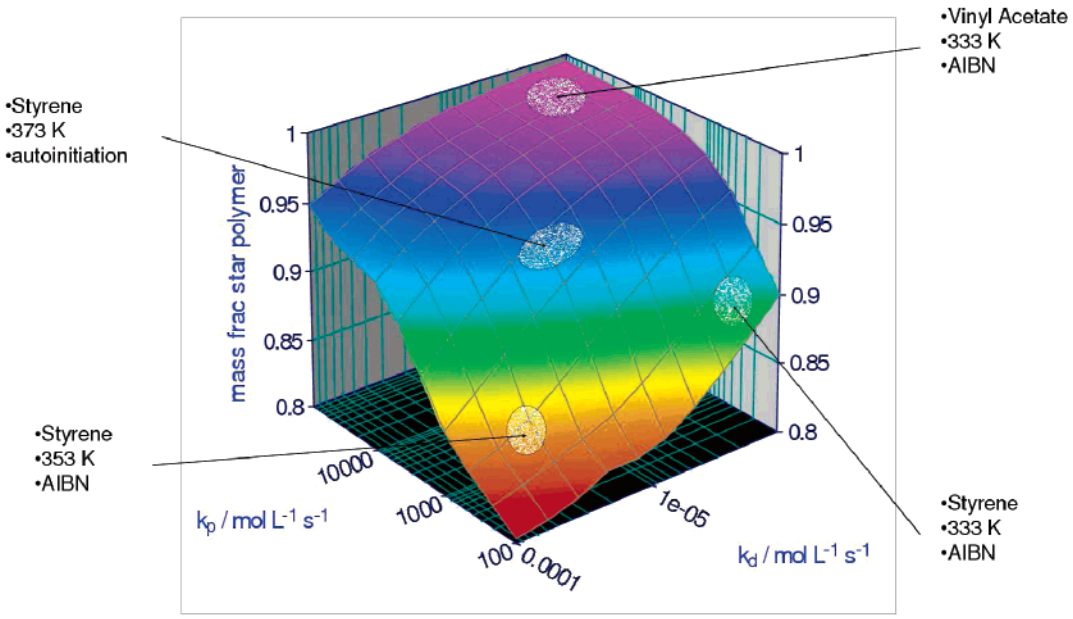

Figure 5. Mass fraction of star polymer (= mass star/(mass star + mass linear) as a function of the propagation rate coefficient, k_p, and the decomposition rate coefficient for the initiator, k_d, after polymerization to 30% conversion. Specific regions have been marked out as corresponding to actual experimental conditions: (1) AIBN initiated polymerization of vinyl acetate at 60 °C; (2) autoinitiated styrene at 100 °C; (3) AIBN-initiated polymerization of styrene at 60 °C; (4) AIBN-initiated polymerization of styrene at 80 °C. This shows a clear relationship between the rate of initiation and the rate of propagation, leading to the differences in the amount of linear chain present in various polymerizations. The simulated data were generated using $c_{\text{RAFT groups}} = 1 \times 10^{-2}$ mol L^{-1} and $c_{\text{AIBN}} = 2 \times 10^{-3}$ mol L^{-1} as fixed values.

Table 3. Parameters Used When Cross-Termination of the Seven-Membered Ring Radical Was Implemented in the PREDICI Simulation

parameter	value	notes
K/L mol^{-1}	1×10^8	*a*
k_{close}/L mol^{-1} s^{-1}	1×10^7	*b*
k_{open}/ s^{-1}	1×10^{-1}	*c*
$\langle k_{\text{t,cross}} \rangle$/L mol^{-1} s^{-1}	1×10^6	*d*

[a] Equilibrium constant, $K = k_{\text{add}}/k_{\text{frag}}$, used for intramolecular RAFT equilibrium. [b] Addition rate coefficient used for intramolecular RAFT equilibrium. [c] Fragmentation coefficient used for intramolecular RAFT equilibrium. [d] Termination rate coefficient used in implementation of cross-termination of seven-membered ring radical and also macroRAFT radicals—this was chosen to be arbitrarily lower than the termination rate coefficient of two propagating radicals ($k_t \approx 10^8$ L mol^{-1} s^{-1}) since if it were of this latter order, essentially no polymerization would occur.[26]

intermolecular and intramolecular addition are respectively given by

$$R_{\text{inter}} = k_\beta c_{\text{RAFT groups}} c_{\text{radicals}}$$

and

$$R_{\text{intra}} = k_{\text{close}} c_{\text{radicals}}$$

Thus, the probability, p_{intra}, of intramolecular rather than intermolecular addition is, in the early stages of the polymerization, close to

$$p_{\text{intra}} = \frac{R_{\text{intra}}}{R_{\text{intra}} + R_{\text{inter}}}$$

$$= \frac{k_{\text{close}}}{k_{\text{close}} + k_\beta c_{\text{RAFT groups}}}$$

$$= \frac{1 \times 10^7}{1 \times 10^7 + 1 \times 10^6 \times 10^{-2}}$$

$$\approx 0.999$$

It is put forward here that the low MW shoulder on the peak due to ideal stars may be due to termination reactions taking place early in the polymerization, whereby creating a population of stars possessing a small number of arms that are oligomeric. For there to be such a low MW shoulder, the termination reactions *must* take place early in the polymerization—if they occurred continuously throughout the polymerization, there would be not such a pronounced shoulder, but rather a less distinct broadening of the MWD. To probe how such a termination reaction as the one depicted in Scheme 4.V might influence an experimental MWD, such a reaction was implemented in a PREDICI simulation. It should be noted at this point that the equilibrium calculated above is unimolecular and that in the modeling scheme employed here intramolecular processes of a star are approximated as bimolecular processes between arms. Additionally, it seems likely that not only the closed ring compound of Scheme 4 forms but also that where a small number of monomer units might have been incorporated into the ring system as a result of propagation events.

A simulation has thus been parametrized using two sets of rate coefficients for the additional reactions depicted in Scheme 4: the two sets of rate coefficients correspond to (a) intramolecular RAFT equilibria with cross-termination of the seven-membered ring-radical species and (b) intramolecular RAFT equilibria without cross-termination of the seven-membered ring-radical species. The results from this are presented in Figure 7. Upon observation of this figure, it can be seen that the MWD corresponding to the system with cross-termination displays a reduction in the amount of material on the high MW side of the peak due to ideal stars. This is because more radicals were consumed in termination reactions early in the polymerization and less were available for the formation of star−star couples. Additionally, the peak due to ideal star molecules in the cross-termination system has shifted to a lower molecular weight than in the non-cross-termination system because, once again, radicals have been consumed early in the polymerization and were not available for arm extension.

Scheme 4. Intramolecular RAFT Equilibria Occurring in the Preequilibrium of Small-Core, Multiarm, R-Group Approach RAFT Polymerization

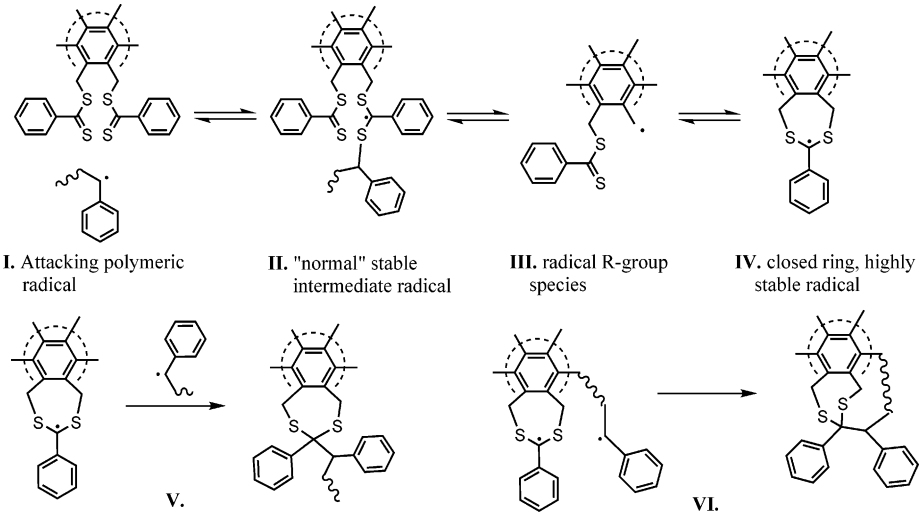

Scheme 5. Small Model of the Larger 4- or 6-Arm RAFT Agent Depicted in Scheme 3, As Used in the Quantum Chemical Calculations of the Equilibrium Constant $K = k_{close}/k_{open}$

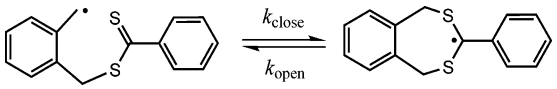

Recall that the model used in this study models all reactions of stars as bimolecular reactions of arms, including intrastar, unimolecular reactions. Therefore, the value of the (bimolecular) equilibrium constant used in the model needs to be higher than the actual, physical, equilibrium constant. It was found that the bimolecular equilibrium constant for the intramolecular RAFT equilibrium needed to be 10^8 L mol^{-1} in order to create a significant low MW shoulder.

While a low molecular weight shoulder creating mechanism resembling the described termination process is tendered as a hypothesis, there are several issues which must be discussed. By allowing cross-termination between a seven-membered ring radical and a propagating radical, one must ask whether cross-termination between intermolecularly formed −S−C•(Z)−S− species (macro-RAFT radicals) and propagating radicals is also possible. When these cross-terminations together with the ring-radical cross-terminations are implemented in a PREDICI simulation (with all other parameters left unchanged), it is found that ring-radical cross-terminated and macro-RAFT radical cross-terminated products are formed with comparable concentrations. If both these cross-termination reaction channels were available in rate-retarded polymerizations, the consequences would be that (a) very large amounts of cross-terminated polymer material would be generated[26] and (b) the rate of the polymerization would be very low (if not completely inhibited) as all propagating and stable intermediate radicals would effectively be terminated. It is clear therefore that the proposed mechanism cannot be completely correct, and there may be other considerations such as that (a) the seven-membered ring radical is less hindered than the macro-RAFT radicals, and therefore terminates more easily, and (b) the termination process only occurs at very low conversions, where short chain lengths would minimize hindrance even further. It must be noted that the low molecular weight shoulder on the MWD can only be formed via a potential cross-termination mechanism in conjunction with a large equilibrium constant for the seven-membered ring intermediate radical.

This section of the current study does however indicate two things. First, that intramolecular RAFT equilibria by themselves have only a subtle effect on the overall kinetics and, second, that some sort of special termination early in the polymerization (and only at this time) might be responsible for low MW shoulders on the peak due to normal star polymer material. It would be illustrative to perform mass spectrometry on the polymer produced in these polymerizations; however, styrene does not have a sufficiently high ionization potential to allow for this. Mass spectrometry might however be used to probe more closely this aspect of the kinetics of, for example, methyl (meth)acrylate star polymerizations. Such experiments are currently underway in our laboratories.

3.4. Effect of Initiator Quantity Variation. Understanding of the results in this section relies on the arguments and example presented in section 3.1. Figure 8 contains a simulated MWD for 4-arm styrene star polymerizations at 80 °C with three different initiator (AIBN) concentrations, $c_{AIBN} = 4 \times 10^{-4}$, 2×10^{-3}, and 1×10^{-2} mol L^{-1} and a RAFT agent concentration of $c_{RAFT\ groups} = 1 \times 10^{-2}$ mol L^{-1}. It can be seen from this that the concentration of initiator has a significant effect on the MWDs. Specifically, it can be seen that as the amount of initiator increases, the relative amount of linear material increases as compared to the amount of star material. This is because with more initiator, proportionally more linear species have the opportunity to bear a radical during the course of the polymerization, and converted monomer is shared out with the linear growth sites. Additionally, as the concentration of initiator increases, there is a very large broadening of the MWDs. This is caused by coupling reactions leading to the formation of multiply joined star polymers. Recalling from section 3.1, we can expect the number of terminated products to be similar to and no more than the number of initiator molecules decomposed. In all but the simulation for the highest initiator concentration, the amount of time which has elapsed is many times the half-life of AIBN at 80 °C ($t_{1/2} \approx 7 \times 10^3$ s), and for that high initiator case, the elapsed time is approximately equal to one half-life. This means that, especially for the case of the highest initiator concentration, the number of coupled species is approaching that of the number of stars in the system, which here is given by $c_{stars} = c_{RAFT}/a = 0.01/4 = 0.0025$ mol L^{-1}, where a is the number of arms.

It is also noteworthy that the positions of all peaks (especially those due to linear material) shift to decreasing molecular weight

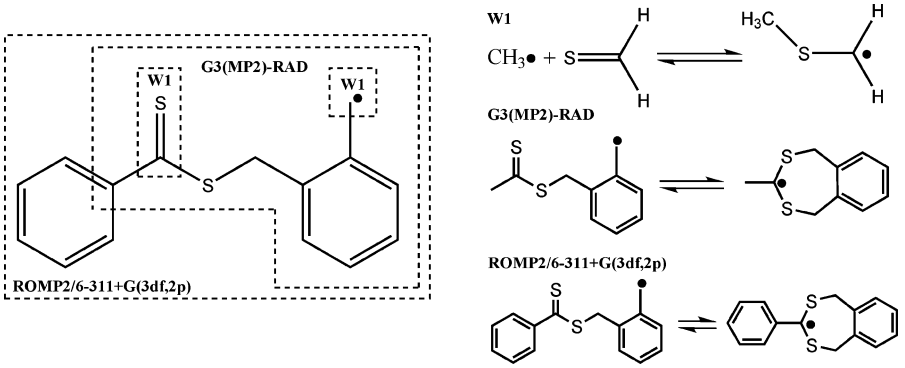

Figure 6. Application of the ONIOM method to approximation of high levels of theory for the current system.

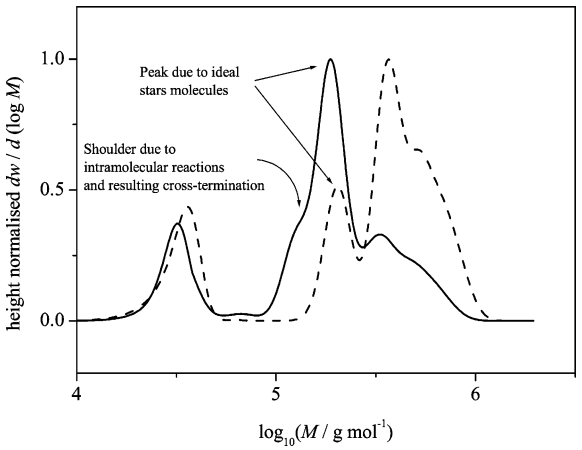

Figure 7. Effect of an intramolecular RAFT equilibrium and cross-termination reaction (see Scheme 4) resulting from a high concentration of intermediate RAFT radicals during the preequilibrium: (—) intramolecular RAFT equilibrium and cross-termination of seven-membered ring radical, showing low molecular weight shoulder on peak due to ideal star molecules; (- - -) intramolecular RAFT equilibrium and *no* cross-termination of seven-membered ring radical. Simulations were parametrized for AIBN initiated 4-arm styrene polymerization at 80 °C. Simulated data are presented for a time of $t = 1 \times 10^5$ s. The parameters used in the additional reactions leading to the curve (—) are given in Table 3. In both simulations, $c_{\text{RAFT groups}} = 1 \times 10^{-2}$ mol L^{-1} and $c_{\text{AIBN}} = 2 \times 10^{-3}$ mol L^{-1}.

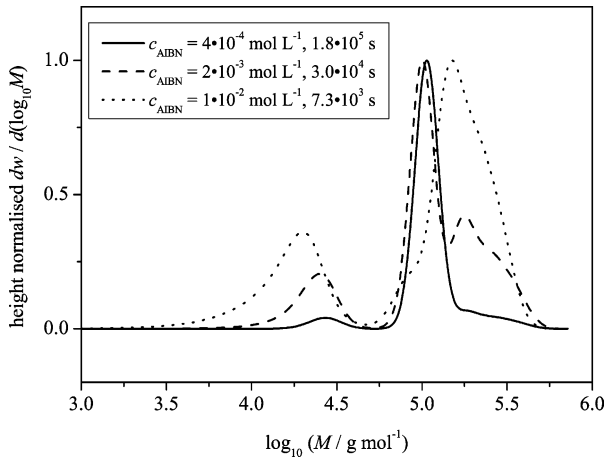

Figure 8. Effect of variation of initial initiator concentration on MWDs. Simulations were parametrized for AIBN initiated 4-arm styrene polymerization at 80 °C. MWDs depict simulations performed to close to 30% conversion. In all simulations $c_{\text{RAFT groups}} = 1 \times 10^{-2}$ mol L^{-1}. It can be seen that an increase in the amount of initiator leads to an increase in the broadness and the size of the peak due to linear chains formed from initiator fragments.

with increasing $c_{\text{AIBN},0}$ even though the conversion is approximately the same. This is an expected deviation from the standard expression for the DP_n of an ideal RAFT polymerization:

$$DP_n = \frac{Xc_{\text{monomer}}}{c_{\text{RAFT}}} \tag{5}$$

where X is the monomer conversion. This deviation occurs because eq 5 fails to take into account conversion on the part of polymeric material whose origin is initiator fragments. Such an effect is particularly prominent with star polymerizations because the initiator-fragment-bound material has a molecular weight significantly different to that of the R-group-bound material since the several of the latter are joined together as a star.

3.5. Effect of Using Rate-Retarded vs Non-Rate-Retarded RAFT Agents. Recall that in the current study, due to a significant body of evidence,[22−26] the cause of rate retardation has been modeled as slow fragmentation of an intermediate RAFT radical, i.e., slow β-scission of the form X−S−C•(Z)−S− → X−S−C(Z)(=S) + Z•. This slow fragmentation causes a reduction in the concentration of propagating radicals (leading to rate retardation) and a reduction in the number of termination events (under the assumption that cross termination is absent).

In Figure 2, the couple fraction was plotted as a function of conversion for rate-retarded and non-rate-retarded RAFT agents. It was noted that the value of the couple fraction was significantly higher for the simulations of non-rate-retarded systems. Such a significant difference in the degree to which stars couple with one another must be observable in the MWDs of experimental systems. Two 4-arm RAFT agents (**II** and **III** in Scheme 3) have been used to study the role of retardation in the synthesis of 4-arm styrene stars; Figure 9 depicts selected MWDs from these experiments. It has been found in the systems studied that the non-rate-retarded RAFT agents lead to MWDs showing a considerably greater degree of structure and broadening than the rate-retarded but otherwise equivalent system. This can be understood by noting that the broadness and continuation of the MWDs up to extremely high molecular weight ($\approx 10^6$ g mol^{-1}) is most likely caused by stars which have coupled to one another by termination events between their arms. This coupling occurs to a far greater extent in the non-rate-retarded system because the radical concentration is far higher than for the rate-retarded system.

As well as the higher degree of coupling observed in the nonretarded system, there may be other factors leading to the distinct differences in the MWDs. Since non-rate-retarded systems experience a greater rate of conversion of monomer into polymer, at a certain conversion, less initiator will have decomposed than at the same conversion of a rate-retarded

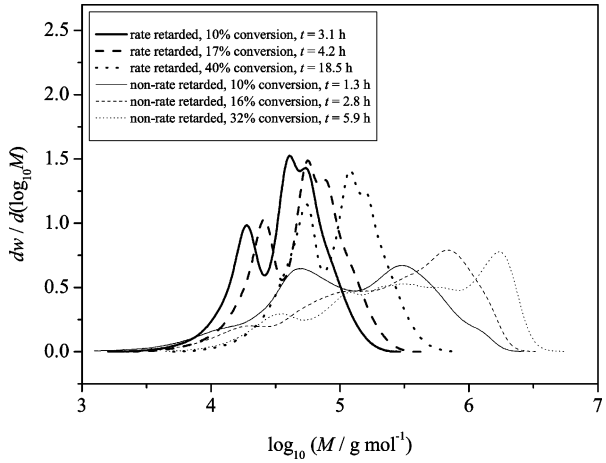

Figure 9. GPC traces from rate-retarded and non-rate-retarded 4-arm RAFT, R-group approach star polymerizations making use of the RAFT agents in Scheme 3, structures II and III. The polymerizations were carried out at 80 °C in bulk styrene under initiation by AIBN. For all experiments, concentrations were close to $c_{\text{RAFT groups}} = 1 \times 10^{-2}$ mol L^{-1} and $c_{\text{AIBN}} = 2 \times 10^{-2}$ mol L^{-1}. Polymerizations which made use of the non-rate-retarding RAFT agent became extremely broad, believed to be caused by termination reactions leading to star−star coupling. These termination reactions are partially reduced in the case of the rate-retarding RAFT agent.

system, meaning that the concentration of linear chains is less for the non-rate-retarded system. Consequently, the average DP_n of nonterminated arms will be larger in the non-rate-retarded system than in the rate-retarded system as a result of monomer to polymer conversion taking place more on star rather than at linear-chain growth sites.

It is worth noting that because there are more linear chains present in the rate-retarded system, differences in the termination kinetics of star polymer radicals vs linear polymer, particularly linear oligomeric radicals, might cause qualitative changes in Figure 2. Chain-length-dependent termination might also be particularly important for the current section of this study, and consequently, we have not sought to simulate full MWDs but have nevertheless understood experimental MWDs in terms of the underlying kinetic model.

From the observations made in this section of the study, it is suggested that while in certain fast propagating systems (e.g., vinyl acetate) the use of a nonretarding RAFT agent might minimize the presence of linear chain impurities, in slower propagating systems, i.e., ones in which several half-lives of initiator decomposition have passed during the course of the polymerization, retardation appears to prevent the formation of couples via reduction of the propagating radical concentration. It should be noted that if retardation occurred predominantly via cross-termination throughout the polymerization rather than slow fragmentation, the rate-retarded systems would be expected to display a greater degree coupling than the non-rate-retarded system; however, this has not been observed in the current experiments.

It must be noted that this section of the study does not rule out the use of non-rate-retarded RAFT agents if other parameters are chosen judicously. Indeed, Rizzardo et al. describe R-group approach systems based on (non-rate retarding) trithiocarbonate RAFT agents which yielded quite narrow MWDs.[63] The crucial difference between those systems and the ones that have been the subject of the current section is that they were performed at high temperature under autoinitiation of styrene, which together result in a low rate of radical delivery but a high propagation rate coefficient. A low rate of radical delivery combined with a high rate of conversion results in a low potential for coupled product formation as well as minimal linear chain formation.

4. Conclusions

The kinetic model described in ref 21 has been used to develop an improved understanding of the kinetics of RAFT, R-group approach synthesized star polymers. It has been found that the type of molecular weight distributions (MWDs) obtained is strongly dependent on the extent of termination reactions in a polymerization since these, along with linear chain forming reactions, are the main avenue for creation of nonstar material leading to structured MWDs. Leading on from this improved understanding, we are able to suggest a set of guidelines for future star polymer syntheses via a RAFT, R-group approach.

Minimal Linear Chain Contaminants. To minimize the quantity of linear polymer in the system, it is important to have a high rate of monomer propagation but a small delivery of radicals to the system. The minimization of linear material, however, must be weighed up against the competing requirement that all RAFT groups are activated and that there is not a large disparity of arm lengths on the resulting stars.

Minimization of Star−Star Coupling via Control of Initiation. Crucial to the prevention of star−star coupling and resulting MWD broadening is the minimization of radical termination events between star molecules. The number of biradical termination events may be no more than the number of initiator decompositions, and as such, minimization of the latter quantity will lead to less broad MWDs. As for the first point, one must still meet the requirement of a fully activated star RAFT agent and sufficiently equal arm lengths.

Minimization of Star−Star Coupling via Intermediate RAFT Radical Stabilization. Another phenomenon capable of preventing termination events is the formation of persistent radicals. Polymer chain extension and termination events have respectively a first-order ($\propto c_{P\bullet}$) and second-order ($\propto c_{P\bullet}^2$) kinetics ($c_{P\bullet}$ is concentration of polymer chain/arm radical). This means that e.g. a 2-fold reduction of $c_{P\bullet}$ will lead to a 2-fold reduction in the rate of polymerization, but a 4-fold reduction in the concentration of coupled products at the conclusion of the polymerization. Therefore, as has been noted in the current study, some systems exhibit less structured MWDs when a rate-retarded RAFT agent is employed.

Minimization of Star−Star Coupling via RAFT Agent Arm Reduction. Our simulations have shown that in otherwise equivalent systems the likelihood of a star being in a star−star couple increases as the number of arms increases. This is due to there being a fixed probability that any one arm is forming a star−star couple and that an increase in the number of arms increases the probability that a *star* is in a star−star couple.

The above points manifest compromises between various aspects of star polymer design via a RAFT, R-group approach. As an example, the importance of a high rate of polymerization must be judged against the requirement of a low degree of star−star coupling. Also, the use of a nonretarding RAFT agent might be entirely justifiable if only a small quantity of initiator will be decomposed, as in the case of vinyl acetate.[19]

Acknowledgment. C.B.-K. and M.H.S. acknowledge funding from the Australian Research Council (ARC) in the form of a Discovery grant. T.P.D. acknowledges receipt of a Federation Fellowship (ARC). The authors are grateful to Mr. Pierre Millard (MCII, University of Bayreuth, Germany) for performing several light scattering gel permeation chromatography analyses of polymer samples. The authors also gratefully

acknowledge generous allocations of computing time on the National Facility of the Australian Partnership for Advanced Computing and the Australian National University Supercomputing Facility. H.C.-M. acknowledges a University of New South Wales Post-Graduate Award.

Appendix. Theory for Star−Star Couples

Previously, a simulation methodology was described in which it was assumed that stars underwent termination reactions to form at most a 2-couple. An improvement of the theory has since been developed and implemented, allowing for the simulation of full MWDs in which stars form arbitrary order couples. This is explained in the current section.

First note that a 2-couple is the structure formed when 2 star molecules couple, a 3-couple the structure when 3 star molecules couple, and so on. For calculation of full MWDs one requires the value of (a) the concentration *n*-couple for each $n = 1, 2, ...$ and (b) the number of star molecules consumed in the formation of those *n*-couples. Therefore, the concentration of an *n*-couple is denoted c_n. The number of arms in an *n*-couple which are chemically responsible for the links is $(n - 1)$. It can be said therefore that the total number of linkages in an *n*-couple is $(n - 1)c_n$, and it is true that

$$\sum_{n=2}^{\infty}(n-1)c_n = c_{\text{termed}}$$

where c_{termed} is the concentration of all terminated species that represent a coupled arm. Dividing by c_{termed}, one arrives at

$$\sum_{n=2}^{\infty}\frac{(n-1)c_n}{c_{\text{termed}}} = 1$$

and it can be written

$$\sum_{n=2}^{\infty}\frac{(n-1)c_n}{c_{\text{termed}}} = 1 = \sum_{n=2}^{\infty}P_n$$

where P_n is the probability that a randomly chosen coupled species (denoted A-coupled in the kinetic model) is in an *n*-couple. Then

$$c_n = \frac{P_n c_{\text{termed}}}{n-1}$$

One can now calculate the concentration, c_n, of *n*-couples as long as we know values for P_n. As already stated, coupling is an anomalous process, and it is not desired to simulate it exactly; therefore, we pick a series of monotonically decreasing P_ns, up to some maximum $n = N$, such that $\sum_{n=2}^{N}P_n = 1$. For example

$$P_n = \begin{cases} 0.4 & n = 2 \\ 0.3 & n = 3 \\ 0.2 & n = 4 \\ 0.1 & n = 5 \\ 0 & n \geq 5 \end{cases} \qquad (6)$$

To calculate the concentration of noncoupled stars (i.e., 1-couples), it is also necessary to know the concentration of star centers, S_n, in each *n*-couple. This is given by

$$S_n = nc_n$$

which is found by substituting in the above expression for c_n. The values of c_n are used to convert a probability distribution of *n*-couples to a concentration distribution. Concentration distributions are then further converted to GPC distributions in the normal way, i.e., by multiplication of the concentration $c(i)$ of each chain-length *i* by i^2. Probability distributions of *n*-couples were generated via the method developed previously, which was the subject of ref 21. The couple probabilities used in all simulations described in the current paper are those given in eq 6.

Supporting Information Available: Section S1 containing the B3LYP/6-31G(d) optimized geometries used in all energy and entropy calculations as well as section S2 containing the kinetic model implemented in PREDICI used in the current study. This material is available free of charge via the Internet at http://pubs.acs.org.

Note Added after ASAP Publication. This article was published ASAP on August 19, 2006. Several modifications have been made to Scheme 2. The correct version was published on August 23, 2006.

References and Notes

(1) Wang, J.-S.; Matyjaszewski, K. *J. Am. Chem. Soc.* **1995**, 5614−5615.
(2) Haddleton, D. M.; Crossman, M. C.; Dana, B. H.; Duncalf, D. J.; Heming, A. M.; Kukulj, D.; Shooter, A. J. *Macromolecules* **1999**, *32*, 2110−2119.
(3) Hawker, C. J.; Bosman, A. W.; Harth, E. *Chem. Rev.* **2001**, *101*, 3661−3688.
(4) Chong, B. Y. K.; Krstina, J.; Le, T. P. T.; Moad, G.; Postma, A.; Rizzardo, E.; Thang, S. H. *Macromolecules* **2003**, *36*, 2256−2272.
(5) Calitz, F. M.; Tonge, M. P.; Sanderson, R. D. *Macromolecules* **2003**, *36*, 5−8.
(6) Moad, G.; Rizzardo, E.; Thang, S. H. *Aust. J. Chem.* **2005**, *58*, 379−410.
(7) Chiefari, J.; Mayadunne, R. T. A.; Moad, C. L.; Moad, G.; Rizzardo, E.; Postma, A.; Skidmore, M. A.; Thang, S. H. *Macromolecules* **2003**, *36*, 2273−2283.
(8) Barner, L.; Barner-Kowollik, C.; Davis, T. P.; Stenzel, M. H. *Aust. J. Chem.* **2004**, *57*, 19−24.
(9) Perrier, S.; Takolpuckdee, P. *J. Polym. Sci., Part A: Polym. Chem.* **2005**, *43*, 5347−5393.
(10) Feng, X.-S.; Pan, C.-Y. *Macromolecules* **2002**, *35*, 2084−2089.
(11) Stenzel-Rosenbaum, M.; Davis, T. P.; Chen, V.; Fane, A. G. *J. Polym. Sci., Part A: Polym. Chem.* **2001**, *39*, 2777−2783.
(12) Matyjaszewski, K.; Miller, P. J.; Pyun, J.; Kickelbick, G.; Diamanti, S. *Macromolecules* **1999**, *32*, 6526−6535.
(13) Radke, W.; Gerbera, J.; Wittmann, G. *Polymer* **2003**, *44*, 519−525.
(14) Pyun, J.; Rees, I.; Fréchet, J. M. J.; Hawker, C. J. *Aust. J. Chem.* **2003,** *56*, 775−782.
(15) Angot, S.; Murthy, K. S.; Taton, D.; Gnanou, Y. *Macromolecules* **1998**, *31*, 7218−7225.
(16) Ueda, J.; Kamigaito, M.; Sawamoto, M. *Macromolecules* **1998**, *31*, 6762−6768.
(17) Jesberger, M.; Barner, L.; Stenzel, M. H.; Malmström, E.; Davis, T. P.; Barner-Kowollik, C. *J. Polym. Sci., Part A: Polym. Chem.* **2003**, *41*, 3847−3861.
(18) Hao, X.; Nilsson, C.; Jesberger, M.; Stenzel, M. H.; Malmström, E.; Davis, T. P.; Östmark, E.; Barner-Kowollik, C. *J. Polym. Sci., Part A: Polym. Chem.* **2004**, *42*, 5877−5890.
(19) Bernard, J.; Favier, A.; Zhang, L.; Nilasaroya, A.; Davis, T. P.; Barner-Kowollik, C.; Stenzel, M. H. *Macromolecules* **2005**, *38*, 5475−5484.
(20) Stenzel, M. H.; Davis, T. P. *J. Polym. Sci., Part A: Polym. Chem.* **2002**, *40*, 4498−4512.
(21) Chaffey-Millar, H.; Busch, M.; Davis, T. P.; Stenzel, M. H.; Barner-Kowollik, C. *Macromol. Theory Simul.* **2005**, *14*, 143−157.
(22) Ah Toy, A.; Vana, P.; Davis, T. P.; Barner-Kowollik, C. *Macromolecules* **2004**, *37*, 744−751.
(23) Barner-Kowollik, C.; Coote, M. L.; Davis, T. P.; Radom, L.; Vana, P. *J. Polym. Sci., Part A: Polym. Chem.* **2003**, *41*, 2828−2832.
(24) Feldermann, A.; Coote, M. L.; Stenzel, M. H.; Davis, T. P.; Barner-Kowollik, C. *J. Am. Chem. Soc.* **2004**, *126*, 15915−15923.
(25) Feldermann, A.; Ah Toy, A.; Davis, T. P.; Stenzel, M. H.; Barner-Kowollik, C. *Polymer* **2005**, *46*, 8448−8457.
(26) Barner-Kowollik, C.; Buback, M.; Charleux, B.; Coote, M. L.; Drache, M.; Fukuda, T.; Goto, A.; Klumpermann, B.; Lowe, A. B.; McLeary,

J.; Moad, G.; Monteiro, M. J.; Sanderson, R. D.; Tonge, M. P.; Vana, P. *J. Polym. Sci., Part A: Polym. Chem.*, in press.
(27) Barner-Kowollik, C.; Quinn, J. F.; Morsley, D. R.; Davis, T. P. *J. Polym. Sci., Part A: Polym. Chem.* **2001**, *39*, 1353−1365.
(28) Le, T. P.; Moad, G.; Rizzardo, E.; Thang, S. H. PCT Int. Appl. WO 9801478, 1998; 88 pp.
(29) Zimm, B. H.; Stockmayer, W. H. *J. Chem. Phys.* **1949**, *17*, 1301−1314.
(30) Radke, W. *Macromol. Theory Simul.* **2001**, *10*, 668−675.
(31) Wulkow, M.; Busch, M.; Davis, T. P.; Barner-Kowollik, C. *J. Polym. Sci., Part A: Polym. Chem.* **2004**, *42*, 1441−1448.
(32) Wulkow, M. *Macromol. Theory Simul.* **1996**, *5*, 393−416.
(33) Buback, M.; Huckestein, B.; Kuchta, F.; Russell, G.; Schmid, E. *Macromol. Chem. Phys.* **1994**, *195*, 2117−2140.
(34) Vana, P.; Davis, T. P.; Barner-Kowollik, C. *Macromol. Theory Simul.* **2002**, *11*, 823−835.
(35) Buback, M.; Kuchta, F. *Macromol. Chem. Phys.* **1997**, *198*, 1455−1480.
(36) Buback, M.; Gilbert, R. G.; Hutchinson, R. A.; Kulperman, B.; Kuchta, F.-D.; Manders, B. G.; O'Driscoll, K. F.; Russell, G. T.; Schweer, J.; *Macromol. Chem. Phys.* **1995**, *196*, 3267−3280.
(37) Patnode, W.; Scheiber, W. J. *J. Am. Chem. Soc.* **1939**, *61*, 3445−3448.
(38) Theis, A.; Davis, T. P.; Stenzel, M. H.; Barner-Kowollik, C. *Polymer* **2006**, *47*, 999−1010.
(39) Coote, M. L. Molecular Orbital Theory for Free-Radical Polymerisation. In *Encyclopedia of Polymer Science and Technology*; Kroschwitz, J. I., Ed.; Wiley: New York, 2004.
(40) Atkins, P.; de Paula, J. *Physical Chemistry;* Oxford University Press: New York, 2001.
(41) Frisch, M. J.; Trucks, G. W.; Schlegel, H. B.; Scuseria, G. E.; Robb, M. A.; Cheeseman, J. R.; Zakrzewski, V. G.; Montgomery, J. A. Jr.; Stratmann, R. E.; Burant, J. C.; Dapprich, S.; Millam, J. M.; Daniels, A. D.; Kudin, K. N.; Strain, M. C.; Farkas, O.; Tomasi, J.; Barone, V.; Cossi, M.; Cammi, R.; Mennucci, B.; Pomelli, C.; Adamo, C.; Clifford, S.; Ochterski, J.; Petersson, G. A.; Ayala, P. Y.; Cui, Q.; Morokuma, K.; Rega, N.; Salvador, P.; Dannenberg, J. J.; Malick, D. K.; Rabuck, A. D.; Raghavachari, K.; Foresman, J. B.; Cioslowski, J.; Ortiz, J. V.; Baboul, A. G.; Stefanov, B. B.; Liu, G.; Liashenko, A.; Piskorz, P.; Komaromi, I.; Gomperts, R.; Martin, R. L.; Fox, D. J.; Keith, T.; Al-Laham, M. A.; Peng, C. Y.; Nanayakkara, A.; Challacombe, M.; Gill, P. M. W.; Johnson, B.; Chen, W.; Wong, M. W.; Andres, J. L.; Gonzalez, C.; Head-Gordon, M.; Replogle, E. S.; Pople, J. A. *Gaussian 98, Revision A.11.3*; Gaussian, Inc.: Pittsburgh, PA, 1998.
(42) Frisch, M. J.; Trucks, G. W.; Schlegel, H. B.; Scuseria, G. E.; Robb, M. A.; Cheeseman, J. R.; Montgomery, J. A., Jr.; Vreven, T.; Kudin, K. N.; Burant, J. C.; Millam, J. M.; Iyengar, S. S.; Tomasi, J.; Barone, V.; Mennucci, B.; Cossi, M.; Scalmani, G.; Rega, N.; Petersson, G. A.; Nakatsuji, H.; a Hada, M.; Ehara, M.; Toyota, K.; Fukuda, R.; Hasegawa, J.; Ishida, M.; Nakajima, T.; Honda, Y.; itao, O.; Nakai, H.; Klene, M.; Li, X.; Knox, J. E.; Hratchian, H. P.; Cross, J. B.; Adamo, C.; Jaramillo, J.; Gomperts, R.; Stratmann, R. E.; Yazyev, O.; Austin, A. J.; Cammi, R.; Pomelli, C.; Ochterski, J. W.; Ayala, P. Y.; Morokuma, K.; Voth, G. A.; Salvador, P.; Dannenberg, J. J.; Zakrzewski, V. G.; Dapprich, S.; Daniels, A. D.; Strain, M. C.; Farkas, O.; Malick, D. K.; Rabuck, A. D.; aghavachari, K.; Foresman, J. B.; Ortiz, J. V.; Cui, Q.; Baboul, A. G.; Clifford, S.; Cioslowski, J.; Stefanov, B. B.; Liu, G.; Liashenko, A.; Piskorz, P.; Komaromi, I.; Martin, R. L.; Fox, D. J.; Keith, T.; Al-Laham, M. A.; Peng, C. Y.; Nanayakkara, A.; Challacombe, M.; Gill, P. M. W.; Johnson, B.; Chen, W.; Wong, M. W.; Gonzalez, C.; Pople, J. A. *Gaussian 03;* Gaussian, Inc.: Pittsburgh, PA, 2003.
(43) Schmidt, M. W.; Baldridge, K. K.; Boatz, J. A.; Elbert, S. T.; Gordon, M. S.; Jensen, J. J.; Koseki, S.; Matsunaga, N.; Nguyen, K. A.; Su, S.; Windus, T. L.; Dupuis, M.; J.; A. M. J. *J. Comput. Chem.* **1993**, *14*, 1347−1363.
(44) Bernhardsson, A.; Berning, A.; Celani, P.; Cooper, D. L.; Deegan, M. J. O.; Dobbyn, A. J.; Eckert, F.; Hampel, C.; Hetzer, G.; Korona, T.; Lindh, R.; Lloyd, A. W.; McNicholas, S. J.; Manby, F. R.; Meyer, W.; Mura, M. E.; Nicklass, A.; Palmieri, P.; Pitzer, R.; Rauhut, G.; Schütz, M.; Stoll, H.; Stone, A. J.; Tarroni, R.; Thorsteinsson, T. MOLPRO 2000.6, 1999. J. A. M. J. *J. Comput. Chem.* **1993**, *14*, 1347−1363.
(45) Izgorodina, E. I.; Coote, M. L. *J. Phys. Chem. A* **2006,** *110*, 2486-2492.
(46) Parthiban, S.; Martin, J. M. L. *J. Chem. Phys.* **2001**, *114*, 6014−6029.
(47) Martin, J. M. L.; de Oliveira, G. *J. Chem. Phys.* **1999**, 1843−1856.
(48) Hong, C.-Y.; You, Y.-Z.; Liu, J.; Pan, C.-Y. *J. Polym. Sci., Part A: Polym. Chem.* **2005**, *43*, 6379−6393.
(49) Goto, A.; Fukuda, T. *Prog. Polym. Sci.* **2004**, *29*, 329−385.
(50) Wang, A. R.; Zhu, S.; Kwak, Y.; Goto, A.; Fukuda, T.; Monteiro, M. S. *J. Polym. Sci., Part A: Polym. Chem.* **2003**, *41*, 2833−2839.
(51) Barner-Kowollik, C.; Vana, P.; Quinn, J. F.; Davis, T. P. *J. Polym. Sci., Part A: Polym. Chem.* **2002**, *40*, 1058−1063.
(52) Barner-Kowollik, C.; Vana, P.; Davis, T. P. *The Kinetics of Radical Polymerization* in *Handbook of Radical Polymerisation*; Matyjaszewski, K., Davis, T. P., Eds.; John Wiley and Sons: New York, 2002; p 208.
(53) Wilemski, G.; Fixman, M. *J. Chem. Phys.* **1973**, *60*, 866−877.
(54) Ortiz-Repiso, M.; Freire, J. J.; Rey, A. *Macromolecules* **1998**, *31*, 8356−8362.
(55) Klenin, K. V.; Langowskia, J. *J. Chem. Phys.* **2004**, *121*, 4951−4961.
(56) Ortiz-Repiso, M.; Rey, A. *Macromolecules* **1998**, *31*, 8363−8369.
(57) *Polymer Handbook*, 4th ed.; Brandrup, J., Immergut, E. H. E., Grulke, A., Eds.; John Wiley and Sons: New York, p II/103.
(58) Hutchinson, R. A.; D.; A. P. J.; McMinn, J. H.; Beuermann, S.; Fuller, R. E.; Jackson, C. *DECHEMA Monogr.* **1995**, *131*, 467−492.
(59) Favier, A.; Barner-Kowollik, C.; Davis, T. P.; Stenzel, M. H. *Macromol. Chem. Phys.* **2004**, *205*, 925−936.
(60) Stenzel, M. H.; Cummins, L.; Roberts, G. E.; Davis, T. R.; Vana, P.; Barner-Kowollik, C. *Macromol. Chem. Phys.* **2003**, *204*, 1160−1168.
(61) Bernard, J.; Favier, A.; Davis, T. P.; Barner-Kowollik, C.; Stenzel, M. H. *Polymer* **2006**, *47*, 1073−1080.
(62) Coote, M. L.; Izgorodina, E. I.; Krenske, E. H.; Busch, M.; Barner-Kowollik, C. *Macromol. Rapid Commun.* **2006**, *27*, 1015−1022.
(63) Mayadunne, R. T. A.; Jeffery, J.; Moad, G.; Rizzardo, E. *Macromolecules* **2003**, *36*, 1505−1513.

MA060964W